

Synchronization Control for Discrete-Time Delayed Complex Cyber-Physical Networks Under False Data Injection Attacks^{*}

Chaoqun Zhu^{*} Xuan Jia^{*} Pan Zhang^{*}

^{*} *Institute of College of Electrical and Information Engineering
University of Lanzhou University of Technology, Lanzhou, 730050,
China (e-mail: chaoqunzhu@yeah.net, jiaxua_cn@icloud.com,
zhangpanlut@163.com).*

Abstract: This paper is concerned with the synchronization control problem for complex cyber-physical networks with mixed delays and false data injection attacks. The polytopic model of closed-loop synchronization error dynamics is established by considering the pattern characteristics of false data injection attacks and input delays, which has essentially different from the traditional handling method. More specifically, the proposed polytopic model utilizes the current state of the closed-loop synchronization error dynamics, thereby facilitating the reduction of possible conservatism. In such a framework, a nonlinear synchronization control method is developed to eliminate the negative impact of cyber attacks, and sufficient conditions are derived to guarantee that the closed-loop synchronization error dynamics are ultimately exponentially bounded. In the meanwhile, the design procedure of the synchronization controller is proposed for underlying complex cyber-physical networks subject to mixed delays and false data injection attacks. Finally, an illustrative example is delivered to demonstrate the effectiveness of the proposed method.

Keywords: Complex cyber-physical networks, false data injection attacks, mixed delays, synchronization control

1. INTRODUCTION

As typical massively interconnected complex systems, complex networks are composed of a large number of interacting individuals or nodes, whose dynamics can be described by a single nonlinear vector field. For example, biological networks, multi-agent systems, Internet networks, transportation networks, neural networks, electric power grids, etc. Gao et al. (2018); Srinivasan et al. (2022); Rakkiyappan et al. (2014); Zafar et al. (2018). Complex cyber-physical networks (CCPNs) can be regarded as a class of complex networks where each network node exchanges information with its neighbor nodes over the shared communication channels. However, the shared communication channels are often vulnerable to external security risks and various network-induced problems, such as cyber attacks Barboni et al. (2018), time delays Chen et al. (2020), and packet dropouts Souza et al. (2016), which bring certain challenges to the security of CCPNs. Although the security problem of networked systems has received increasing attention in the past few years Wen et al. (2017); Cetinkaya et al. (2015); Tan et al. (2020), there are still few investigations for complex networks. Usually, false data injection (FDI) attacks can inject malicious data to worsen or destabilize the performance of

a dynamical system. In CCPNs, the attackers attempt to modify the data that are communicated between network nodes and the controller for the disruption. For example, FDI attackers penetrate several network nodes and then CCPNs to launch an attack Wen et al. (2017). In Peng et al. (2019), the FDI attacks are utilized to manipulate the trusted network nodes by injecting malicious data. In Zhou et al. (2023), the FDI attacks may cause the actuator to malfunction by the injection of false data, and the sampled-data control method is discussed for the synchronization control of complex dynamical networks with actuator saturation. In general, the existence of FDI attacks may cause the failure of synchronization control, and even collapse complex networks when more network nodes are attacked, which motivates current investigation for CCPNs subject to FDI attacks.

From the viewpoint of detection and estimation of cyber attacks, some interesting results are obtained for complex networks, see e.g. Mousavinejad et al. (2019); Ju et al. (2020); Musleh et al. (2019). To mention a few, the authors in Mousavinejad et al. (2019) discuss the detection problem of cyber attacks in vehicle systems. In Musleh et al. (2019), the main criteria for developing detection algorithms are proposed for the smart grids under FDI attacks. However, the above results are only involved in the detection method without considering the negative impact of cyber attacks on the synchronization performance of complex networks. Recently, various synchronization control strategies have been presented for the complex

^{*} This work was supported in part by the National Natural Science Foundation of China under Grants 62363024, 61863026, in part by the Major Science and Technology Special Project of Gansu Province under Grant 21ZD4GA028.

network under cyber attacks. For instance, a resilient consensus algorithm is proposed to defend the F-local FDI attacks for CCPNs Fu et al. (2019). In He et al. (2018), the authors design an impulsive synchronization controller for the multi-agent systems under FDI attacks, and further analyze the synchronization performance of the systems. A hybrid-driven sampling control scheme is presented to ensure the synchronization performance of complex networks under cyber attacks Shi et al. (2020). Unfortunately, there are much attention has been focused on designing security control strategy for CCPNs subject to cyber attacks so far, while very few results have been available on the synchronization control issue with simultaneous consideration of network-induced effects and cyber attacks. Consequently, it is another research motivation to shorten this gap.

Due to the complex couplings of communication networks, the problem of time delays is inevitable, which is a great challenge for the synchronization control of complex networks. By now, some preliminary results have been addressed for complex networks subject to both cyber attacks and time delays, see e.g. Kazemy et al. (2021); Lee and Park (2019); Qu and Pang (2020). Among them, the authors in Kazemy et al. (2021) present a master-slave synchronization control method for delayed neural networks under cyber attacks. In Lee and Park (2019), the sampled-data control scheme is provided to achieve the synchronization of complex dynamical networks with time delays under cyber attacks. In Qu and Pang (2020), a set-membership state estimation scheme is designed for artificial neural networks subject to time delays and FDI attacks to achieve optimal estimation performance. However, most of the existing results have been obtained for complex networks with single-type time delays, such as state delay, input delay, or output delay, while the synchronization control issue has not been sufficiently explored for the situation of mixed delays (e.g. time-varying input delays and distributed state delays). To address the aforementioned research gap, a theoretical synchronization control framework is proposed for CCPNs with both mixed delays and cyber attacks.

In response to the above discussions, this paper is devoted to the investigation of synchronization control problems for CCPNs with mixed delay and FDI attacks. The main contributions of this paper can be summarized as follows.

- (1) A novel polytopic model is introduced to characterize FDI attacks and input delays, then the nonlinear state-feedback synchronization controller is proposed for CCPNs subject to mixed delays and FDI attacks.
- (2) With the energy-constrained FDI attacks strategy, an analytical expression of the closed-loop synchronization error dynamics (CLSEDs) is developed and sufficient conditions are derived for the ultimate boundedness of CLSEDs.

Paper Organization: Section II is the problem description and preliminaries. In Section III, the design procedure of the synchronization controller is proposed for CCPNs with the effects of mixed delays and FDI attacks. An illustrative example is provided in Section IV to demonstrate the effectiveness of the proposed results. Finally, Section V

concludes the paper and discusses future research directions.

The notations used in this paper are standard and expressed as Table 1:

Table 1. Notations.

Notations	Expression
\mathcal{R}^n	n -dimensional Euclidean space
$\mathcal{R}^{n \times n}$	$n \times n$ real matrices
$\mathcal{R}(l)$	The l -th row of matrix \mathcal{R}
\mathcal{R}_n^+	The symmetric positive definite matrix \mathcal{R}
R^T	The transpose of the matrix R
$P > 0$	Matrix P is positive definite
$P \geq 0$	Matrix P is positive semi-definite
$\ x\ _2$	The two-norm
$\ x\ _\infty$	The infinite-norm
\otimes	The Kronecker product
$*$	Symmetric entry
$I/0$	Identity matrix / zero matrix
Δ	The differential operator
$Sym(T)$	$Sym(T) = T^T + T$
$\lambda_{\min}(T)$	The smallest eigenvalues of Matrix T
$diag\{\cdot\}$	The diagonal matrix
I_N	The $N \times N$ identity matrix

2. PROBLEM DESCRIPTION

Considering a class of CCPNs consisting of N identically coupled nodes as follows:

$$\begin{aligned}
 x_i(k+1) &= Ax_i(k) + A_d \sum_{l=1}^{+\infty} \mu_l x_i(k-l) \\
 &\quad + \sum_{j=1}^N \tilde{l}_{ij} \Gamma x_j(k) + Bu_i(k - \tau_k), \\
 x(\theta) &= \phi_i(\theta), \theta \in (-\infty, 0], i = 1, 2, \dots, N. \quad (1)
 \end{aligned}$$

where $x_i(k) \in \mathcal{R}^n$, $u_i(k) \in \mathcal{R}^n$ and $\phi(\theta) \in \mathcal{R}^n$ denote the state vector, the control input, and the initial condition, respectively. τ_k is the time-varying delay satisfying $\tau_m \leq \tau_k \leq \tau_M$ (where τ_m and τ_M are positive integers, denoting the lower and upper bounds of τ_k). $\sum_{l=1}^{+\infty} \mu_l x_i(k-l)$ indicates infinite distributed state delay, Γ denote the inner-coupling matrix, and $L = (\tilde{l}_{ij})_{N \times N}$ is a matrix representing the outer-coupling configuration with $\tilde{l}_{ij} \geq 0$ ($i \neq j$) and $\sum_{j=1}^N \tilde{l}_{ij} = 0$. A , A_d , and $B \in \mathcal{R}^n$ are known constant matrices with appropriate dimensions.

As shown in Fig. 1, the model of FDI attacks will be introduced for CCPNs. In this paper, the FDI attacks [23] aim to contaminate control input with false data and thus threaten the system security, and the actual control input after FDI attacks can be expressed as follows:

$$\tilde{u}_i(k - \tau_k) = u_i(k - \tau_k) + f(u_i(k - \tau_k)). \quad (2)$$

where $f(u_i(k - \tau_k)) \in \mathcal{R}^n$ is the vector of the FDI attacks.

For FDI attacks $f(u_i(k - \tau_k))$, the following assumption is given.

Assumption 1. For a constant matrix F , FDI attacks signals $f(u_i(k - \tau_k))$ satisfy the following sector conditions:

$$f^T(u_i(k - \tau_k)) F [f(u_i(k - \tau_k)) - u_i(k - \tau_k)] \leq 0.$$

where F is a constant matrix with appropriate dimensions.

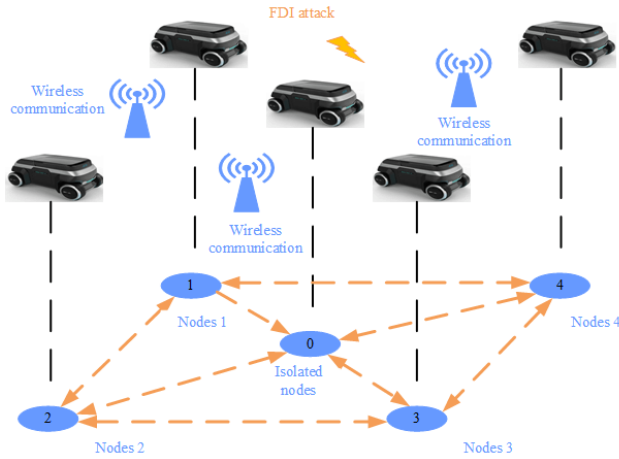


Fig. 1. Illustration of CCPNs under FDI attacks.

Then, the model of CCPNs (1) under FDI attacks is obtained as follows:

$$\begin{aligned} x_i(k+1) &= Ax_i(k) + A_d \sum_{l=1}^{+\infty} \mu_l x_i(k-l) \\ &\quad + \sum_{j=1}^N \tilde{l}_{ij} \Gamma x_j(k) + Bu_i(k-\tau_k) \\ &\quad + Bf(u_i(k-\tau_k)), \\ x(\theta) &= \phi_i(\theta), \theta \in (-\infty, 0], i = 1, 2, \dots, N. \end{aligned} \quad (3)$$

In this paper, the following form of the isolated node is considered:

$$\begin{aligned} s(k+1) &= As(k) + A_d \sum_{l=1}^{+\infty} \mu_l s(k-l), \\ s(\theta) &= \phi(\theta), \theta \in (-\infty, 0]. \end{aligned} \quad (4)$$

where $s(k) \in \mathcal{R}^n$ denote the state vector of isolated node.

Define the synchronization error as follows:

$$e_i(k) = x_i(k) - s(k), \tilde{\phi}_i(\theta) = \phi_i(\theta) - \phi(\theta).$$

Then, the following matrices and notations are introduced:

$$\begin{aligned} \tilde{A} &= I_N \otimes A, \tilde{A}_d = I_N \otimes A_d, \\ \tilde{B} &= I_N \otimes B, \tilde{F} = I_N \otimes F, \tilde{L} = L \otimes \Gamma, \\ e(k) &= [e_1^T(k) \cdots e_N^T(k)]^T, \\ \tilde{\phi}(\theta) &= [\tilde{\phi}_1^T(\theta) \cdots \tilde{\phi}_N^T(\theta)]^T, \\ u(k-\tau_k) &= [u_1^T(k-\tau_k) \cdots u_N^T(k-\tau_k)]^T, \\ \tilde{f}(e(k)) &= [\tilde{f}^T(e_1(k)) \cdots \tilde{f}^T(e_N(k))]^T. \end{aligned}$$

According to (3) and (4), as well as the above definition, the CLSEDs can be obtained as follows:

$$\begin{aligned} e(k+1) &= (\tilde{A} + \tilde{L})e(k) + \tilde{A}_d \sum_{l=1}^{+\infty} \mu_l e(k-l) \\ &\quad + \tilde{B}u(k-\tau_k) + \tilde{B}\tilde{f}(u(k-\tau_k)), \\ e(\theta) &= \tilde{\phi}(\theta), \theta \in (-\infty, 0]. \end{aligned} \quad (5)$$

To achieve the synchronization control of CCPNs, a synchronization controller is employed as follows:

$$u_i(k) = K_i e_i(k), i = 1, 2, \dots, N. \quad (6)$$

where $K_i \in \mathcal{R}^{n \times n}$ is the synchronization control gain matrices of the i -th individual node.

For the proposed synchronization error dynamics (5), Assumptions are given as follows:

Assumption 2. Chen and Wang (2020) For a given scalar $\mu_i > 0$ ($i = 1, 2, \dots$), there is a positive scalar $0 < \lambda \leq 1$, such that the following inequality holds

$$\begin{aligned} \sum_{i=1}^{+\infty} \mu_i \lambda^{-i} &< \sum_{j=1}^{+\infty} \sum_{i=1}^j \mu_i \lambda^{-i} \\ &< \sum_{l=1}^{+\infty} \sum_{j=1}^l \sum_{i=1}^j \mu_i \lambda^{-i} < +\infty. \end{aligned}$$

Assumption 3. There exists a time sequence

$$0 = k_1 < \tilde{k}_1 < k_2 < \tilde{k}_2 < \cdots < k_r < \tilde{k}_r = k^* \leq \tau_M,$$

such that the following relationship holds

$$k - \tau_k < 0, k \in \tilde{\Upsilon}; k - \tau_k \geq 0, k \in \hat{\Upsilon} \cup [k^*, +\infty).$$

where $\tilde{\Upsilon} = [k_1, \tilde{k}_1) \cup [k_2, \tilde{k}_2) \cup \cdots \cup [k_r, \tilde{k}_r)$, $\hat{\Upsilon} = [\tilde{k}_1, k_2) \cup [\tilde{k}_2, k_3) \cup \cdots \cup [\tilde{k}_{r-1}, k_r)$.

Under Assumption 3, there is no control input signal in $\tilde{\Upsilon}$ (i.e., $u(k-\tau_k) = 0$). Then, the CLSEDs are obtained as follows:

$$\begin{aligned} e(k+1) &= (\tilde{A} + \tilde{L})e(k) + \tilde{A}_d \sum_{l=1}^{+\infty} \mu_l e(k-l), \\ e(\theta) &= \tilde{\phi}(\theta), \theta \in (-\infty, 0], k \in \tilde{\Upsilon}. \end{aligned} \quad (7)$$

To handle the FDI attacks within the interval $\hat{\Upsilon}$, the synchronization error dynamics (5) are equivalent to

$$\begin{aligned} e(k+1) &= (\tilde{A} + \tilde{L})e(k) + \tilde{A}_d \sum_{l=1}^{+\infty} \mu_l e(k-l) \\ &\quad + \tilde{B}u(k-\tau_k) + \tilde{B}\tilde{f}(u(k-\tau_k)), \\ e(\theta) &= \tilde{\phi}(\theta), \theta \in (-\infty, 0], k \in \hat{\Upsilon}. \end{aligned} \quad (8)$$

where $K = \text{diag}\{K_1, K_2, \dots, K_N\}$.

According to Assumption 1, for the vector-valued function $\tilde{f}(e(k-\tau_k))$, the following sector condition holds

$$\tilde{f}^T(e(k-\tau_k)) \tilde{F} [\tilde{f}(e(k-\tau_k)) - e(k-\tau_k)] \leq 0, k \in \hat{\Upsilon}. \quad (9)$$

Before proceeding further, the following Lemmas are introduced, which will be helpful in subsequent developments.

Lemma 4. Zhou (2013) For the given integer $v \geq 1$, and $z \in R^{\tilde{v}}$, such that $\|z\|_\infty \leq 1$, where $\tilde{v} = v2^{v-1}$. If there exist the elements in the set E_v defined as E_i ($i \in [1, 2^v]$), where E_v is a diagonal matrix of $v \times v$ with diagonal elements of 1 or 0, then the real function f_v has the following form

$$\begin{aligned} f_v(0) &= 0, \\ f_v(i) &= \begin{cases} f_v(i-1) + 1, & E_i + E_j \neq I_v, \forall j \in [1, i] \\ f_v(j), & E_i + E_j = I_v, \exists j \in [1, i] \end{cases}, \end{aligned}$$

and $f(u(k)) \in \text{co}\{E_i u(k) + \tilde{E}_i^- z(k) : i \in [1, 2^v]\}$ holds for any $u(k) \in \mathcal{R}^v$, where ‘co’ is the convex hull, $\tilde{E}_i^- \in \mathcal{R}^{v \times v}$, $\tilde{E}_i^- = e_{2^{v-1}, i} \otimes D_i^-$ and $E_i^- = I - E_i$.

Lemma 5. Solomon and Fridman (2013); Chen et al. (2018) For the given state vector $x_i \in \mathcal{R}^n$, if there exist the positive definite matrix $Z \in \mathcal{R}^{n \times n}$, and the positive scalars $\mu_i \geq 0$ and $\lambda_j \geq 0$ ($i, j = 1, 2, \dots$), then the following linear inequalities hold

$$\begin{aligned}
& \left(\sum_{i=1}^{+\infty} \mu_i x_i \right)^T Z \left(\sum_{i=1}^{+\infty} \mu_i x_i \right) \\
& \leq \left(\sum_{i=1}^{+\infty} \mu_i \lambda_i^- \right) \left(\sum_{i=1}^{+\infty} \mu_i \lambda_i x_i^T Z x_i \right), \\
& \left(\sum_{j=1}^{+\infty} \sum_{i=1}^j \mu_j x_i \right)^T Z \left(\sum_{j=1}^{+\infty} \sum_{i=1}^j \mu_j x_i \right) \\
& \leq \left(\sum_{j=1}^{+\infty} \sum_{i=1}^j \mu_j \lambda_i^- \right) \\
& \times \left(\sum_{j=1}^{+\infty} \sum_{i=1}^j \mu_j \lambda_i x_i^T Z x_i \right).
\end{aligned}$$

Lemma 6. Seuret et al. (2015) If the symmetric matrix $0 < R \in \mathcal{R}_n^+$ is given, such that, for the scalar $\tau_M \geq 1$ and time variables e in $[-\tau_M, 0] \rightarrow \mathcal{R}^n$, the following matrices inequality holds

$$\begin{aligned}
& \sum_{i=-\tau_M+1}^0 g^T(i) R g(i) \\
& \geq \frac{1}{\tau_M} \begin{bmatrix} \pi_0 \\ \pi_1 \end{bmatrix}^T \begin{bmatrix} R & 0 \\ 0 & 3\varphi_\tau R \end{bmatrix} \begin{bmatrix} \pi_0 \\ \pi_1 \end{bmatrix}.
\end{aligned}$$

where $g(i) = e(i+1) - e(i)$, $\pi_0 = e(k) - e(k - \tau_M)$, $\pi_1 = e(k) + e(k - \tau_M) - \varphi_\tau \sum_{i=-\tau_M}^0 e(i)$ and $\varphi_\tau = (\tau_M + 1)/(\tau_M - 1)$, $\tau_M > 1$, $\varphi_1 = 1$.

Lemma 7. Seuret et al. (2015) If there exist the matrices $M \in \mathcal{R}^{n \times m}$, $S_1 \in \mathcal{R}_n^+$ and $S_2 \in \mathcal{R}_m^+$, such that, for $\begin{bmatrix} S_1 & M \\ M^T & S_2 \end{bmatrix} \geq 0$ and any $a \in (0, 1)$ the following reciprocally convex combination inequality holds:

$$\begin{bmatrix} \frac{1}{a} S_1 & 0 \\ 0 & \frac{1}{1-a} S_2 \end{bmatrix} \geq \begin{bmatrix} S_1 & M \\ M & S_2 \end{bmatrix}.$$

Next, the matrices $D \in \mathcal{R}^{\vec{v} \times n}$, $G \in \mathcal{R}^{\vec{v} \times n}$ and $O \in \mathcal{R}^{\vec{v} \times n}$ are defined, and denote that

$$\begin{aligned}
z(k) &= D e(k) + G \sum_{l=1}^{+\infty} \mu_l e(k-l) \\
&+ O \sum_{j=1}^{+\infty} \mu_j \sum_{i=k-j}^{k-1} e(i), \quad (10)
\end{aligned}$$

where $v \geq 1$ is a given integer, and $\vec{v} = v2^{v-1}$.

It is assumed that $z(k)$ satisfies the following conditions for all $[k^*, +\infty)$:

$$\|z(k)\|_\infty \leq 1, \quad k \in [k^*, +\infty). \quad (11)$$

Then, according to Lemma 4, the following $\tilde{f}(e(k - \tau_k))$ is obtained:

$$\begin{aligned}
\tilde{f}(e(k - \tau_k)) &= \sum_{y=1}^{2^v} \varpi_y^k [E_y e(k - \tau_k) \\
&+ E_y^- z(k)], \quad k \in [k^*, +\infty). \quad (12)
\end{aligned}$$

where $y \in [1, 2^v]$, $\varpi_y^k \geq 0$, $\sum_{y=1}^{2^v} \varpi_y^k = 1$, E_y is a diagonal matrix of $v \times v$ with diagonal elements of 1 or 0, and $E_i^- = I - E_i$.

Substitute (11) into (12), which yields

$$\begin{aligned}
\tilde{f}(e(k - \tau_k)) &= \sum_{y=1}^{2^v} \varpi_y^k [E_y e(k - \tau_k) + E_y^- (D e(k) \\
&+ O \sum_{j=1}^{+\infty} \mu_j \sum_{i=k-j}^{k-1} e(i) \\
&+ G \sum_{l=1}^{+\infty} \mu_l e(k-l))] , \quad k \in [k^*, +\infty). \quad (13)
\end{aligned}$$

Substituting (13) into (8), it is obtained the CLSEDs as follows:

$$\begin{aligned}
e(k+1) &= \sum_{y=1}^{2^v} \varpi_y^k \left\{ \left(\tilde{A} + \tilde{L} + \tilde{B} E_y^- D \right) e(k) \right. \\
&+ \tilde{B} (I + E_y) K e(k - \tau_k) \\
&+ \left(\tilde{A}_d + \tilde{B} E_y^- G \right) \sum_{l=1}^{+\infty} \mu_l e(k-l) \\
&\left. + \tilde{B} E_y^- O \sum_{j=1}^{+\infty} \mu_j \sum_{i=k-j}^{k-1} e(i) \right\}, \\
e(\theta) &= \tilde{\phi}(\theta), \quad \theta \in (-\infty, 0], \quad k \in [k^*, +\infty). \quad (14)
\end{aligned}$$

Remark 8. To ensure the less conservativeness of the time-varying nonlinear input $\tilde{f}(e(k - \tau_k))$, some terms (e.g., $E_y^- G \sum_{l=1}^{+\infty} \mu_l e(k-l)$, $\tilde{B} E_y^- O \sum_{j=1}^{+\infty} \mu_j \sum_{i=k-j}^{k-1} e(i)$) are introduced to match the infinite distributional delays when coping with the polytopic model (13). In addition, it is worth noting that the proposed polytopic model (13) by utilizing current error $e(k)$ differs from the sectorial condition of Chen et al. (2020) to deal with time-varying nonlinearities, which are caused by the combination of mixed delays and FDI attacks.

3. MAIN RESULTS

This paper aims at designing a synchronization controller to guarantee that the CLSEDs (14) are ultimately exponentially bounded. To facilitate post-processing work, the following matrices and notations are introduced:

$$\tilde{\tau}_k = \tau_k + 1, \quad \hat{\tau}_k = \tau_M - \tau_k + 1, \quad \tilde{\tau} = \tau_M + 1,$$

$$\begin{aligned}
\varepsilon_0(k) &= \left[\sum_{l=1}^{+\infty} \mu_l e^T(k-l) \sum_{j=1}^{+\infty} \mu_j \sum_{i=k-\tau}^{k-1} e^T(i) \right. \\
&\left. e(k+1) - e(k) \right]^T,
\end{aligned}$$

$$\varepsilon_1(k) = \left[e^T(k) \quad e^T(k - \tau_k) \quad e^T(k - \tau_M) \quad 1/\tilde{\tau}_k \sum_{i=k-\tau_k}^k e^T(i) \quad 1/\hat{\tau}_k \sum_{i=k-\tau_k}^{k-\tau_k} e^T(i) \quad \varepsilon_0^T(k) \right]^T,$$

$$\varepsilon_2(k) = \left[e^T(k) \quad e^T(k - \tau_k) \quad e^T(k - \tau_M) \quad 1/\tilde{\tau} \sum_{i=k-\tau}^k e^T(i) \quad \varepsilon_0^T(k) \quad u^T(k - \tau_k) \right]^T,$$

$$\varepsilon_3(k) = \left[e^T(k) \quad e^T(k - \tau_M) \quad 1/\tilde{\tau} \sum_{i=k-\tau}^k e^T(i) \quad \varepsilon_0^T(k) \right]^T,$$

$$\Gamma_1 = \begin{bmatrix} I & 0 & 0 & 0 & 0 & 0 & 0 & I \\ 0 & -I & -I & \tilde{\tau}_k I & \hat{\tau}_k I & 0 & 0 & 0 \\ \kappa I & 0 & 0 & 0 & 0 & -I & I & 0 \end{bmatrix},$$

$$\Gamma_2 = \begin{bmatrix} I & 0 & 0 & 0 & 0 & 0 & 0 & 0 \\ -I & -I & 0 & \tilde{\tau}_k I & \hat{\tau}_k I & 0 & 0 & 0 \\ 0 & 0 & 0 & 0 & 0 & 0 & I & 0 \end{bmatrix},$$

$$\Gamma_3 = \begin{bmatrix} I & 0 & 0 & 0 & 0 & 0 & I & 0 \\ 0 & 0 & -I & \tilde{\tau} I & 0 & 0 & 0 & 0 \\ \kappa I & 0 & 0 & 0 & -I & I & 0 & 0 \end{bmatrix},$$

$$\Gamma_4 = \begin{bmatrix} I & 0 & 0 & 0 & 0 & 0 & 0 & 0 \\ -I & 0 & 0 & \tilde{\tau} I & 0 & 0 & 0 & 0 \\ 0 & 0 & 0 & 0 & 0 & I & 0 & 0 \end{bmatrix},$$

$$\Gamma_5 = \begin{bmatrix} I & 0 & 0 & 0 & 0 & I \\ 0 & -I & \tilde{\tau} I & 0 & 0 & 0 \\ \kappa I & 0 & 0 & -I & I & 0 \end{bmatrix},$$

$$\Gamma_6 = \begin{bmatrix} I & 0 & 0 & 0 & 0 & 0 \\ 0 & -I & \tilde{\tau}I & 0 & 0 & 0 \\ 0 & 0 & 0 & 0 & I & 0 \end{bmatrix},$$

$$\Phi_1 = \begin{bmatrix} I & -I & 0 & 0 & 0 & 0 & 0 & 0 \\ I & I & 0 & -2I & 0 & 0 & 0 & 0 \\ 0 & I & -I & 0 & 0 & 0 & 0 & 0 \\ 0 & I & I & 0 & -2I & 0 & 0 & 0 \end{bmatrix},$$

$$\Phi_2 = [\kappa I \ 0 \ 0 \ 0 \ 0 \ -I \ 0 \ 0],$$

$$\Phi_3 = \begin{bmatrix} I & -I & 0 & 0 & 0 & 0 & 0 & 0 \\ 0 & I & -I & 0 & 0 & 0 & 0 & 0 \end{bmatrix},$$

$$\Phi_4 = \begin{bmatrix} I & 0 & -I & 0 & 0 & 0 & 0 & 0 \\ I & 0 & I & -2I & 0 & 0 & 0 & 0 \end{bmatrix},$$

$$\Phi_5 = [\kappa I \ 0 \ 0 \ 0 \ 0 \ -I \ 0 \ 0],$$

$$\Phi_6 = \begin{bmatrix} I & -I & 0 & 0 & 0 & 0 \\ I & I & -2I & 0 & 0 & 0 \end{bmatrix},$$

$$\Phi_7 = [\kappa I \ 0 \ 0 \ -I \ 0 \ 0],$$

$$\Phi_8 = [\tau_M I \ -I \ 0 \ 0], \Phi_9 = [\kappa I \ 0 \ 0 \ -I],$$

$$R_\beta = R_{\beta 1} + R_{\beta 2}, \bar{R}_\beta = \bar{R}_{\beta 1} + \bar{R}_{\beta 2},$$

$$\kappa = \sum_{i=1}^{+\infty} \mu_i, \tilde{\kappa}_\beta = \sum_{i=1}^{+\infty} \mu_i \lambda_\beta^{-i}, \sigma = \sum_{i=1}^{+\infty} i \mu_i,$$

$$\tilde{\sigma}_\beta = \sum_{j=1}^{+\infty} \sum_{i=1}^j \mu_j \lambda_\beta^{-i}, \text{Sym}(T) = T^T + T,$$

$$\varphi_1 = \frac{\lambda_2^{\tau_M} - 1}{\lambda_2 - 1}, \varphi_{2\beta} = \sum_{j=1}^{+\infty} \sum_{i=1}^j \mu_j \lambda_\beta^{-i},$$

$$\varphi_{3\beta} = \sum_{l=1}^{+\infty} \sum_{j=1}^l \sum_{i=1}^j \mu_l \lambda_\beta^{i-1},$$

$$\varphi_4 = \frac{(1 - \lambda_2) \tau_M - \lambda_2 + \lambda_2^{\tau_M + 1}}{(\lambda_2 - 1)^2}, \beta = 1, 2.$$

For the convenience of subsequent presentation, let us introduce the following piecewise Lyapunov-like functional and the definition of boundedness.

The following form of piecewise Lyapunov-like functions is defined:

$$V(k) = \begin{cases} V_1(k), & k \in [k^*, +\infty) \\ V_2(k), & k \in [0, k^*) \end{cases}. \quad (15)$$

where

$$\begin{aligned} V_\beta(k) &= \eta^T(k) P_\beta \eta(k) \\ &+ \sum_{i=k-\tau}^{k-1} \lambda_\beta^{k-i-1} e^T(i) Q_\beta e(i) \\ &+ \sum_{j=1}^{+\infty} \mu_j \sum_{i=k-j}^{k-i} \lambda_\beta^{k-i-1} e^T(i) S_{\beta 1} e(i) \\ &+ \sum_{l=1}^{+\infty} \mu_l \sum_{j=1}^l \sum_{i=k-j}^{k-1} \lambda_\beta^{k-i-1} e^T(i) S_{\beta 2} e(i) \\ &+ \tau_M \sum_{j=-\tau}^{-1} \sum_{i=k+j}^{k-1} \lambda_\beta^{k-i-1} g^T(i) \\ &\times (R_{\beta 1} + R_{\beta 2}) g(i) \\ &+ \sum_{l=1}^{+\infty} \mu_l \sum_{j=1}^l \sum_{i=k-j}^{k-1} \lambda_\beta^{k-i-1} g^T(i) Z_\beta g(i), \\ P_\beta &> 0, Q_\beta > 0, S_{\beta 1} > 0, S_{\beta 2} > 0, R_{\beta 1} > 0, \\ R_{\beta 2} &> 0, Z_\beta > 0, 0 < \lambda_1 \leq 1, \lambda_2 > 1, \\ \beta &= 1, 2, g(k) = e(k+1) - e(k) \text{ and } \eta(k) = \\ &\left[e^T(k) \sum_{i=k-\tau}^{k-1} e^T(i) \sum_{j=1}^{+\infty} \mu_j \sum_{i=k-\tau}^{k-1} e^T(i) \right]^T. \end{aligned}$$

Definition 9. Zhou (2013) For the given scalar $0 < \pi < 1$, if there exist scalars $0 < \lambda_1 \leq 1$ and $\lambda_2 > 1$, such that the following inequality holds

$$V_1(k) \leq \lambda_1^{k-k^*} \left[\pi \lambda_2^{k^*} V_2(0) \right], k \in [k^*, +\infty). \quad (16)$$

Then, the CLSEDs (14) are exponentially bounded.

Theorem 10. For the given positive scalars π , $\lambda_1 \leq 1$, $\lambda_2 > 1$, the synchronization controller gain K , and the positive integer $k^* \geq 1$, if there exist the matrices $D \in \mathcal{R}^{\tilde{v} \times n}$, $G \in \mathcal{R}^{\tilde{v} \times n}$, $O \in \mathcal{R}^{\tilde{v} \times n}$, $M_1 \in \mathcal{R}^{2n \times 2n}$, $M_2 \in \mathcal{R}^{n \times n}$, $T_{ij} \in \mathcal{R}^{n \times n}$, the positive definite matrices $Z_\beta \in \mathcal{R}^{n \times n}$, $S_{\beta j} \in \mathcal{R}^{n \times n}$, $R_{\beta j} \in \mathcal{R}^{n \times n}$, $P_\beta \in \mathcal{R}^{3n \times 3n}$, $Q_\beta \in \mathcal{R}^{n \times n}$ ($i = 1, 2, 3, j, \beta = 1, 2$), and the positive definite diagonal matrix $\tilde{F} \in \mathcal{R}^{nN \times nN}$, such that, for $\tau_k, \forall y \in [1, 2^v]$, and $\forall d \in [1, \tilde{v}]$, the following matrices inequalities hold:

$$\begin{aligned} \Lambda_1 &= \begin{bmatrix} \bar{R}_1 & M_1 \\ M_1^T & \bar{R}_1 \end{bmatrix} > 0, \\ \Lambda_2 &= \begin{bmatrix} R_{21} & M_2 \\ M_2^T & R_{21} \end{bmatrix} > 0, \end{aligned} \quad (17)$$

$$\begin{aligned} \Xi_1 &= \Gamma_1^T P_1 \Gamma_1 - \lambda_1 \Gamma_2^T P_1 \Gamma_2 - \lambda_1^T \Phi_1^T \Lambda_1 \Phi_1 \\ &- \Phi_2^T (Z_1 / \tilde{\sigma}_1) \Phi_2 + \text{Sym}(T_1 \Sigma_1) + \Psi_1 < 0, \end{aligned} \quad (18)$$

$$\begin{aligned} \Xi_2 &= \Gamma_3^T P_2 \Gamma_3 - \lambda_2 (\Gamma_4^T P_2 \Gamma_4 + \Phi_3^T \Lambda_2 \Phi_3 + \Phi_4^T R_{22}^T \Phi_4) \\ &- \Phi_5^T (Z_2 / \tilde{\sigma}_2) \Phi_5 + \text{Sym}(T_2 \Sigma_2 + T_4 \Sigma_4) \\ &+ \Psi_2 < 0, \end{aligned} \quad (19)$$

$$\begin{aligned} \Xi_3 &= \Gamma_5^T P_1 \Gamma_5 - \lambda_2 \Gamma_6^T P_2 \Gamma_6 - \lambda_2 \Phi_6^T R_2^T \Phi_6 \\ &- \Phi_7^T (Z_2 / \tilde{\sigma}_2) \Phi_7 + \text{Sym}(T_3 \Sigma_3) + \Psi_3 < 0, \end{aligned} \quad (20)$$

$$\begin{cases} P_1 \leq \pi P_2, Q_1 \leq \pi Q_2, S_{1j} \leq \pi S_{2j} \\ R_{1j} \leq \pi R_{2j} (j = 1, 2), Z_1 \leq \pi Z_2 \end{cases}, \quad (21)$$

$$\Xi_4(d) = \begin{bmatrix} 1/\pi \lambda_2^{k^*} & \Omega_{(d)} \\ \Omega_{(d)}^T & \text{diag}\{P_1, 0\} + \Psi_4 / \lambda_1 \end{bmatrix} \geq 0. \quad (22)$$

where

$$\Omega_{(d)} = [D_{(d)} \ 0 \ G_{(d)} \ O_{(d)}],$$

$$\begin{aligned} \Psi_1 &= \text{diag}\{Q_1 + \kappa S_{11} + \sigma S_{12}, 0, -\lambda_1^{\tau_M} Q_1, 0, \\ &0, -S_{11} / \tilde{\kappa}_1, -S_{12} / \tilde{\sigma}_1, \tau_M^2 R_1 + \sigma Z_1\}, \end{aligned}$$

$$\begin{aligned} \Psi_2 &= \text{diag}\{Q_2 + \kappa S_{21} + \sigma S_{22}, 0, -\lambda_2^{\tau_M} Q_2, 0, \\ &-S_{21} / \tilde{\kappa}_2, -S_{22} / \tilde{\sigma}_2, \tau_M^2 R_2 + \sigma Z_2, 0\}, \end{aligned}$$

$$\begin{aligned} \Psi_3 &= \text{diag}\{Q_2 + \kappa S_{21} + \sigma S_{22}, -\lambda_2^{\tau_M} Q_2, 0, \\ &-S_{21} / \tilde{\kappa}_2, -S_{22} / \tilde{\sigma}_2, \tau_M^2 R_2 + \sigma Z_2\}, \end{aligned}$$

$$\begin{aligned} \Psi_4 &= \text{diag}\{0, (\lambda_1^{\tau_M} / \tau_M) Q_1, S_{12} / \tilde{\sigma}_1, S_{11} / \tilde{\kappa}_1\} \\ &+ (2\lambda_1^{\tau_M} / \tilde{\tau}) \Phi_8^T R_1 \Phi_8 + (1 / \tilde{\sigma}_1) \Phi_9^T Z_1 \Phi_9, \end{aligned}$$

$$T_1 = [T_{11}^T \ 0 \ 0 \ 0 \ 0 \ 0 \ 0 \ T_{12}^T]^T,$$

$$T_2 = [T_{21}^T \ 0 \ 0 \ 0 \ 0 \ 0 \ T_{22}^T \ 0]^T,$$

$$T_3 = [T_{31}^T \ 0 \ 0 \ 0 \ 0 \ T_{32}^T]^T,$$

$$T_4 = [0 \ 0 \ 0 \ 0 \ 0 \ 0 \ \tilde{F}^T]^T,$$

$$\begin{aligned} \Sigma_1 &= [\tilde{A} + \tilde{L} + \tilde{B} E_y^- D - I \ \tilde{B} (I + E_y) K \ 0 \ 0 \\ &0 \ \tilde{A}_d + \tilde{B} E_y^- G \ \tilde{B} E_y^- O - I] \end{aligned}$$

$$\Sigma_2 = \begin{bmatrix} \tilde{A} + \tilde{L} - I & 2\tilde{B}K & 0 & 0 \\ \tilde{A}_d & 0 & -I & -\tilde{B} \end{bmatrix}$$

$$\Sigma_3 = \begin{bmatrix} \tilde{A} + \tilde{L} - I & 0 & 0 & \tilde{A}_d & 0 & -I \end{bmatrix}$$

$$\Sigma_4 = \begin{bmatrix} 0 & K & 0 & 0 & 0 & 0 & -I \end{bmatrix}$$

$$\bar{R}_1 = \text{diag} \{R_{11}, 3R_{11}\}, R_2^T = \text{diag} \{R_2, 3\varphi_\tau R_2\}$$

$$R_{22}^T = \text{diag} \{R_{22}, 3\varphi_\tau R_{22}\}$$

Then, for any $\phi(k) \in [0, +\infty)$, Lyapunov-like function $V_2(k)$ satisfying $V_2(0) \leq 1$, and the CLSEDs (14) are ultimately exponentially bounded.

Proof. For $\forall k \in [0, +\infty)$, define the $\Delta V(k)$ as follows:

$$\Delta V_\beta(k) = V_\beta(k+1) - \lambda_\beta V_\beta(k), \quad \beta = 1, 2. \quad (23)$$

By applying Lemma 5 to (23), one obtains

$$\begin{aligned} \Delta V_\beta(k) &\leq \eta^T(k+1) P_\beta \eta(k+1) - \lambda_\beta \eta^T(k) P_\beta \eta(k) \\ &+ e^T(k) (Q_\beta + \kappa S_{\beta 1} + \sigma S_{\beta 2}) e(k) + g^T(k) \\ &\times (\tau_M^2 R_\beta + \sigma Z_\beta) g(k) \\ &- \lambda_\beta^\tau e^T(k - \tau_M) Q_\beta e(k - \tau_M) \\ &- \varsigma_1^T(k) (S_{\beta 1} / \tilde{\kappa}_\beta) \varsigma_1(k) - \varsigma_2^T(k) (S_{\beta 2} / \tilde{\sigma}_\beta) \varsigma_2(k) \\ &- \tau_M \tilde{\lambda}_\beta \sum_{i=k-\tau}^{k-1} g^T(i) R_\beta g(i) \\ &- \varsigma_3^T(k) (Z_\beta / \tilde{\sigma}_\beta) \varsigma_3(k). \end{aligned} \quad (24)$$

where $\tilde{\lambda}_1 = \lambda_1^{\tau_M}$, $\tilde{\lambda}_2 = \lambda_2$, $\varsigma_1(k) = \sum_{l=1}^{+\infty} \mu_l e(k-l)$, $\varsigma_2(k) = \sum_{j=1}^{+\infty} \sum_{i=1}^j \mu_j e(k-i)$, and $\varsigma_3(k) = \sum_{j=1}^{+\infty} \sum_{i=1}^j \mu_j g(k-i)$.

Noting that the facts $R_2 > 0$, $R_{22} > 0$, $R_2^T = \text{diag} \{R_2, 3\varphi_\tau R_2\}$, and $R_{22}^T = \text{diag} \{R_{22}, 3\varphi_\tau R_{22}\}$, and applying Lemma 6 for them, such that, for $e(k)$ in $[-\tau_M, 0] \rightarrow \mathcal{R}^n$, $\tau_M \geq 1$, the following matrix inequalities hold:

$$\begin{aligned} \tau_M \sum_{i=k-\tau_M}^{k-1} g^T(i) R_{22} g(i) \\ \geq \varepsilon_2^T(k) \Phi_4^T R_{22}^T \Phi_4 \varepsilon_2(k), \end{aligned} \quad (25)$$

$$\begin{aligned} \tau_M \sum_{i=k-\tau_M}^{k-1} g^T(i) R_2 g(i) \\ \geq \varepsilon_3^T(k) \Phi_6^T R_2^T \Phi_6 \varepsilon_3(k). \end{aligned} \quad (26)$$

Noting the facts $\sum_{i=k-\tau_M}^{k-1} (*) = \sum_{i=k-\tau_k}^{k-1} (*) + \sum_{i=k-\tau_M}^{k-\tau_k-1} (*)$, $R_{\beta j} > 0$, and using the Lemma 6 and the Lemma 7 to (17), then one has

$$\begin{aligned} \tau_M \sum_{i=k-\tau_M}^{k-1} g^T(i) R_{11} g(i) \\ \geq \varepsilon_1^T(k) \Phi_1^T \Lambda_1 \Phi_1 \varepsilon_1(k), \end{aligned} \quad (27)$$

$$\begin{aligned} \tau_M \sum_{i=k-\tau_M}^{k-1} g^T(i) R_{21} g(i) \\ \geq \varepsilon_2^T(k) \Phi_3^T \Lambda_2 \Phi_3 \varepsilon_2(k). \end{aligned} \quad (28)$$

Considering matrices $T_1, T_2, T_3, \Sigma_1, \Sigma_2$ and Σ_3 , from (7), (8), and (14) it is obtained that

$$2\varepsilon_1^T(k) T_1 \Sigma_1 \varepsilon_1(k) = 0, \quad k \in [k^*, +\infty), \quad (29)$$

$$2\varepsilon_2^T(k) T_2 \Sigma_2 \varepsilon_2(k) = 0, \quad k \in \tilde{\Upsilon}, \quad (30)$$

$$2\varepsilon_3^T(k) T_3 \Sigma_3 \varepsilon_3(k) = 0, \quad k \in \hat{\Upsilon}. \quad (31)$$

Furthermore, it follows from sector condition (9) that

$$-2\varepsilon_2^T(k) T_4 \Sigma_4 \varepsilon_2(k) \geq 0, \quad k \in \tilde{\Upsilon}. \quad (32)$$

Considering (18), (27), (29), $\Delta V_1(k)$ and $\sum_{j=1}^{+\infty} \sum_{i=1}^j \mu_j g(k-i) = \kappa e(k) - \sum_{i=1}^{+\infty} \mu_j e(k-i)$, one eventually obtains

$$\begin{aligned} \Delta V_1(k) &\leq \sum_{y=1}^{2^v} \varpi_y^k \varepsilon_1^T(k) \\ &\times \Xi_1 \varepsilon_1(k), \quad k \in [k^*, +\infty). \end{aligned} \quad (33)$$

Similarly, according to (19), (26), and (28), it follows from $\Delta V_2(k)$, (30) and (32) that

$$\Delta V_2(k) \leq \varepsilon_2^T(k) \Xi_2 \varepsilon_2(k), \quad k \in \hat{\Upsilon}. \quad (34)$$

In addition, by considering (20), (26), and (31), it is obtained

$$\Delta V_2(k) \leq \varepsilon_3^T(k) \Xi_3 \varepsilon_3(k), \quad k \in \tilde{\Upsilon}. \quad (35)$$

If (17)-(20) in Theorem 10 holds under τ_k and $\forall y \in [1, 2^v]$, it follows from (33)-(35) that

$$V_1(k+1) \leq \lambda_1 V_1(k), \quad k \in [k^*, +\infty), \quad (36)$$

$$V_2(k+1) \leq \lambda_2 V_2(k), \quad k \in [0, k^*). \quad (37)$$

Considering (35), (36), and (20), which yields

$$V_1(k) \leq \pi V_2(k), \quad k \geq 0. \quad (38)$$

According to (35)-(37), it is obtained

$$V_1(k) \leq \lambda_1^{k-k^*} \left[\pi \lambda_2^{k^*} V_2(0) \right], \quad k \in [k^*, +\infty). \quad (39)$$

In accordance with Lemma 5, note the following facts:

$$\sum_{j=1}^{+\infty} \mu_j \sum_{i=k-j}^{k-1} r(i) \geq \sum_{j=1}^{+\infty} \mu_j r(k-j), \quad (40)$$

$$\sum_{l=1}^{+\infty} \mu_l \sum_{j=1}^l \sum_{i=k-j}^{k-1} r(i) \geq \sum_{l=1}^{+\infty} \mu_l \sum_{j=1}^l r(k-j). \quad (41)$$

where $r(i) > 0$ is real functions.

Applying Lemma 5 and Lemma 6 to (22), one has

$$\begin{aligned} V_1(k) &\geq \tilde{\eta}^T(k) [\text{diag} \{P_1, 0\} + \Psi_4 / \lambda_1] \\ &\times \tilde{\eta}(k), \quad k \in [k^*, +\infty). \end{aligned} \quad (42)$$

where $\tilde{\eta}(k) = \left[\eta^T(k) \sum_{l=1}^{+\infty} \mu_l e^T(k-l) \right]^T$.

By using the Schur complementary lemma to (22), it is eventually obtained

$$\begin{aligned} \text{diag} \{P_1, 0\} + \Psi_4 / \lambda_1 &\geq \pi \lambda_2^{k^*} \Omega_{(d)}^T \\ &\times \Omega_{(d)}, \quad d \in [1, \vec{v}]. \end{aligned} \quad (43)$$

Considering (39), (42) and (43), it is obtained

$$\begin{aligned} |z_d(k)|^2 &= \tilde{\eta}^T(k) \Omega_{(d)}^T \Omega_{(d)} \tilde{\eta}(k) \\ &\leq \left(1 / \left(\pi \lambda_2^{k^*} \right) \right) V_1(k) \\ &\leq V_2(0), \quad d \in [1, \vec{v}], \quad k \in [k^*, +\infty). \end{aligned} \quad (44)$$

Then, according to Definition 9, for any $\phi(k) \in [0, +\infty)$, $V_2(0) \leq 1$, the CLSEDs (14) are ultimately exponentially bounded. It completes the proof.

For a given parameterized synchronization control gain K , sufficient conditions are provided in Theorem 10 for ensuring the ultimately exponentially bounded of the CLSEDs (14) in $[k^*, +\infty)$. Next, we want to solve the design problem of synchronization control gain K based on Theorem 10.

Theorem 11. For the given positive scalars π , $\lambda_1 \leq 1$, $\lambda_2 > 1$, the positive integer $k^* \geq 1$, and the scalars $\delta_i \neq 0 (i = 1, 2, 3)$, if there exist matrices $\tilde{D} \in \mathcal{R}^{\tilde{v} \times n}$, $\tilde{G} \in \mathcal{R}^{\tilde{v} \times n}$, $\tilde{O} \in \mathcal{R}^{\tilde{v} \times n}$, $\tilde{M}_1 \in \mathcal{R}^{2n \times 2n}$, $\tilde{M}_2 \in \mathcal{R}^{n \times n}$, $X \in \mathcal{R}^{n \times n}$, $Y \in \mathcal{R}^{n \times n}$, the positive definite matrices $\tilde{Z}_\beta \in \mathcal{R}^{n \times n}$, $\tilde{S}_{\beta j} \in \mathcal{R}^{n \times n}$, $\tilde{R}_{\beta j} \in \mathcal{R}^{n \times n}$, $\tilde{Q}_\beta \in \mathcal{R}^{n \times n}$, $\tilde{P}_\beta \in \mathcal{R}^{3n \times 3n}$ ($\beta, j = 1, 2$), and the positive definite diagonal matrix $\tilde{F} \in \mathcal{R}^{nN \times nN}$, such that, for $\tau_k, \forall y \in [1, 2^v]$, and $\forall d \in [1, \tilde{v}]$, the following matrices inequalities hold:

$$\begin{aligned} \tilde{\Lambda}_1 &= \begin{bmatrix} \hat{R}_1 & \tilde{M}_1 \\ \tilde{M}_1^T & \hat{R}_1 \end{bmatrix} > 0, \\ \tilde{\Lambda}_2 &= \begin{bmatrix} \tilde{R}_{21} & \tilde{M}_2 \\ \tilde{M}_2^T & \tilde{R}_{21} \end{bmatrix} > 0, \end{aligned} \quad (45)$$

$$\begin{aligned} \tilde{\Xi}_1 &= \Gamma_1^T \tilde{P}_1 \Gamma_1 - \lambda_1 \Gamma_2^T \tilde{P}_1 \Gamma_2 - \lambda_1^{\tau_M} \Phi_1^T \tilde{\Lambda}_1 \Phi_1 + \tilde{\Psi}_1 \\ &\quad - \Phi_2^T \left(\tilde{Z}_1 / \tilde{\sigma}_1 \right) \Phi_2 + \text{Sym} \left(\tilde{T}_1 \tilde{\Sigma}_1 \right) < 0, \end{aligned} \quad (46)$$

$$\begin{aligned} \tilde{\Xi}_2 &= \Gamma_3^T \tilde{P}_2 \Gamma_3 - \lambda_2 \left(\Gamma_4^T \tilde{P}_2 \Gamma_4 + \Phi_3^T \tilde{\Lambda}_2 \Phi_3 + \Phi_4^T \tilde{R}_{22} \Phi_4 \right) \\ &\quad - \Phi_5^T \left(\tilde{Z}_2 / \tilde{\sigma}_2 \right) \Phi_5 + \text{Sym} \left(\tilde{T}_2 \tilde{\Sigma}_2 + \tilde{T}_4 \tilde{\Sigma}_4 \right) \\ &\quad + \tilde{\Psi}_2 < 0, \end{aligned} \quad (47)$$

$$\begin{aligned} \tilde{\Xi}_3 &= \Gamma_5^T \tilde{P}_1 \Gamma_5 - \lambda_2 \Gamma_6^T \tilde{P}_2 \Gamma_6 - \lambda_2 \Phi_6^T \tilde{R}_{22} \Phi_6 + \tilde{\Psi}_3 \\ &\quad - \Phi_7^T \left(\tilde{Z}_2 / \tilde{\sigma}_2 \right) \Phi_7 + \text{Sym} \left(\tilde{T}_3 \tilde{\Sigma}_3 \right) < 0, \end{aligned} \quad (48)$$

$$\begin{cases} \tilde{P}_1 \leq \pi \tilde{P}_2, \tilde{Q}_1 \leq \pi \tilde{Q}_2, \tilde{S}_{1j} \leq \pi \tilde{S}_{2j} \\ \tilde{R}_{1j} \leq \pi \tilde{R}_{2j} (j = 1, 2), \tilde{Z}_1 \leq \pi \tilde{Z}_2 \end{cases}, \quad (49)$$

$$\tilde{\Xi}_4(d) \begin{bmatrix} 1/\pi \lambda_2^{k^*} & \tilde{\Omega}_{(d)} \\ \tilde{\Omega}_{(d)}^T & \text{diag} \left\{ \tilde{P}_1, 0 \right\} + \tilde{\Psi}_4 / \lambda_1 \end{bmatrix} \geq 0. \quad (50)$$

where

$$\tilde{\Omega}_{(d)} = \left[\tilde{D}_{(d)} \ 0 \ \tilde{G}_{(d)} \ \tilde{O}_{(d)} \right],$$

$$\begin{aligned} \tilde{\Psi}_1 &= \text{diag} \left\{ \tilde{Q}_1 + \kappa \tilde{S}_{11} + \sigma \tilde{S}_{12}, 0, -\lambda_1^{\tau_M} \tilde{Q}_1, 0, \right. \\ &\quad \left. 0, -\tilde{S}_{11} / \tilde{\kappa}_1, -\tilde{S}_{12} / \tilde{\sigma}_1, \tau_M^2 \tilde{R}_1 + \sigma \tilde{Z}_1 \right\}, \end{aligned}$$

$$\begin{aligned} \tilde{\Psi}_2 &= \text{diag} \left\{ \tilde{Q}_2 + \kappa \tilde{S}_{21} + \sigma \tilde{S}_{22}, 0, -\lambda_2^{\tau_M} \tilde{Q}_2, 0, \right. \\ &\quad \left. -\tilde{S}_{21} / \tilde{\kappa}_2, -\tilde{S}_{22} / \tilde{\sigma}_2, \tau_M^2 \tilde{R}_2 + \sigma \tilde{Z}_2, 0 \right\}, \end{aligned}$$

$$\begin{aligned} \tilde{\Psi}_3 &= \text{diag} \left\{ \tilde{Q}_2 + \kappa \tilde{S}_{21} + \sigma \tilde{S}_{22}, -\lambda_2^{\tau_M} \tilde{Q}_2, 0, \right. \\ &\quad \left. -\tilde{S}_{21} / \tilde{\kappa}_2, -\tilde{S}_{22} / \tilde{\sigma}_2, \tau_M^2 \tilde{R}_2 + \sigma \tilde{Z}_2 \right\}, \end{aligned}$$

$$\begin{aligned} \tilde{\Psi}_4 &= \text{diag} \left\{ 0, (\lambda_1^{\tau_M} / \tau_M) \tilde{Q}_1, \tilde{S}_{12} / \tilde{\sigma}_1, \tilde{S}_{11} / \tilde{\kappa}_1 \right\} \\ &\quad + (2\lambda_1^{\tau_M} / \tilde{\tau}) \Phi_8^T \tilde{R}_1 \Phi_8 + (1/\tilde{\sigma}_1) \Phi_9^T \tilde{Z}_1 \Phi_9, \end{aligned}$$

$$\tilde{T}_1 = [I \ 0 \ 0 \ 0 \ 0 \ 0 \ 0 \ \delta_1 I]^T,$$

$$\tilde{T}_2 = [I \ 0 \ 0 \ 0 \ 0 \ 0 \ \delta_2 I \ 0]^T,$$

$$\tilde{T}_3 = [I \ 0 \ 0 \ 0 \ 0 \ 0 \ \delta_3 I]^T,$$

$$\tilde{T}_4 = [0 \ 0 \ 0 \ 0 \ 0 \ 0 \ 0 \ I]^T,$$

$$\begin{aligned} \tilde{\Sigma}_1 &= \left[\left(\tilde{A} + \tilde{L} - I \right) X^T + \tilde{B} E_y^- \tilde{D} \ \tilde{B} (I + E_y) Y \right. \\ &\quad \left. 0 \ 0 \ 0 \ \tilde{A}_d X^T + \tilde{B} E_y^- \tilde{G} \ \tilde{B} E_y^- \tilde{O} \ -X^T \right], \end{aligned}$$

$$\begin{aligned} \tilde{\Sigma}_2 &= \left[\left(\tilde{A} + \tilde{L} - I \right) X^T \ 2\tilde{B} Y \ 0 \ 0 \right. \\ &\quad \left. \tilde{A}_d X^T \ 0 \ -X^T \ -\tilde{B} \tilde{F} \right], \end{aligned}$$

$$\tilde{\Sigma}_3 = \left[\left(\tilde{A} + \tilde{L} - I \right) X^T \ 0 \ 0 \ \tilde{A}_d X^T \ 0 \ -X^T \right],$$

$$\tilde{\Sigma}_4 = [0 \ Y \ 0 \ 0 \ 0 \ 0 \ 0 \ -\tilde{F}],$$

$$\hat{R}_1 = \text{diag} \left\{ \tilde{R}_1, 3\tilde{R}_1 \right\}, \bar{R}_2^T = \text{diag} \left\{ \tilde{R}_2, 3\varphi_\tau \tilde{R}_2 \right\},$$

$$\bar{R}_{22}^T = \text{diag} \left\{ \tilde{R}_{22}, 3\varphi_\tau \tilde{R}_{22} \right\}.$$

Then, for any initial condition $\phi(k) \in [0, +\infty)$, $V_2(0) \leq 1$, the CLSEDs (14) are exponentially bounded, and the corresponding synchronization controller can be determined by $K = YX^{-T}$.

Proof. Using the variable substitution method, let $\bar{X} = \text{diag} \{X, X, X\}$, $P_\beta = \bar{X}^{-1} \tilde{P}_\beta \bar{X}^{-T}$, $Q_\beta = X^{-1} \tilde{Q}_\beta X^{-T}$, $S_{\beta j} = X^{-1} \tilde{S}_{\beta j} X^{-T}$, $R_{\beta j} = X^{-1} \tilde{R}_{\beta j} X^{-T}$, $Z_\beta = X^{-1} \tilde{Z}_\beta X^{-T}$, ($\beta, j = 1, 2$), $T_{i1} = X^{-1}$, $T_{i2} = \delta_i X^{-1}$ ($i = 1, 2, 3$), $M_1 = \tilde{X}^{-1} \tilde{M}_1 \tilde{X}^{-T}$, ($\tilde{X} = \text{diag} \{X, X\}$), $K = YX^{-T}$, $M_2 = X^{-1} \tilde{M}_2 X^{-T}$, $\tilde{F} = \tilde{F}^{-T}$, $D = \tilde{D}X^{-T}$, $G = \tilde{G}X^{-T}$, $O = \tilde{O}X^{-T}$. Substitute them into (17)-(22), which yields (45)-(50). This completes the proof.

Remark 12. In Theorem 11, the design problem of the synchronization controller is investigated for CCPNs under FDI attacks. It is worth noting that the existing results mostly utilize the paradigm-bounded model to describe FDI attacks for the simplicity of design, see e.g. Shi et al. (2017); Fu et al. (2019). However, in practice, this kind of modeling method of FDI attacks may bring some conservatism to the synchronization performance of CCPNs. To ensure less conservativeness, the polytopic model (13) is utilized to deal with the FDI attacks of CCPNs. In comparison with available results, it is the first time that the polytopic model has been used to discuss the synchronization problem for CCPNs with mixed delays and FDI attacks.

If there does not exist any input delay τ_k in CCPNs (14), the corresponding CLSEDs are obtained as follows:

$$\begin{aligned} e(k+1) &= \sum_{s=1}^{2^v} \varpi_s^k \left\{ \left(\tilde{A} + \tilde{L} + \tilde{B} E_s^- D \right. \right. \\ &\quad \left. \left. + \tilde{B} K E_s \right) e(k) \right. \\ &\quad \left. + \left(\tilde{A}_d + \tilde{B} E_s^- G \right) \sum_{i=1}^{+\infty} \mu_i e(k-i) \right. \\ &\quad \left. + \tilde{B} E_s^- O \sum_{j=1}^{+\infty} \mu_j \sum_{i=k-j}^{k-1} e(i) \right\}, \\ e(\theta) &= \tilde{\phi}(\theta), \theta \in (-\infty, 0], k \in [0, +\infty). \end{aligned} \quad (51)$$

Define the Lyapunov-like function as follows:

$$\begin{aligned} \vec{V}(k) &= \vec{\eta}^T(k) \text{diag}\{X^{-1}, X^{-1}\} \vec{P} \\ &\times \text{diag}\{X^{-T}, X^{-T}\} \vec{\eta}(k) \\ &+ \sum_{j=1}^{+\infty} \mu_j \sum_{i=k-j}^{k-1} \lambda_1^{k-i-1} e^T(i) X^{-1} \tilde{S}_1 X^{-T} e(i) \\ &+ \sum_{l=1}^{+\infty} \mu_l \sum_{j=1}^l \sum_{i=k-j}^{k-1} \lambda_1^{k-i-1} e^T(i) X^{-1} \tilde{S}_2 X^{-T} \\ &\times e(i) + \sum_{l=1}^{+\infty} \mu_l \sum_{j=1}^l \sum_{i=k-j}^{k-1} \lambda_1^{k-i-1} y^T(i) \\ &\times X^{-1} \tilde{Z} X^{-T} y(i) \end{aligned}$$

where $\vec{\eta}(k) = \left[e^T(k) \sum_{j=1}^{+\infty} \mu_j \sum_{i=k-j}^{k-1} e^T(i) \right]^T$. Then, the controller design of CCPNs (14) is implemented without input delay τ_k .

Corollary 13. For the given positive scalars $\lambda_1 \leq 1$, $\lambda_2 > 1$, and the scalars $\delta \neq 0$, if there exist matrices $\vec{D} \in R^{\vec{v} \times n}$, $\vec{G} \in R^{\vec{v} \times n}$, $\vec{O} \in R^{\vec{v} \times n}$, $X \in R^{n \times n}$, $Y \in R^{n \times n}$, the positive definite matrices $\vec{Z} \in R^{n \times n}$, $\vec{S}_1 \in R^{n \times n}$, $\vec{S}_2 \in R^{n \times n}$, $\vec{P} \in R^{2n \times 2n}$, such that, for $\tau_k, \forall y \in [1, 2^v]$, and $\forall d \in [1, \vec{v}]$, the following matrices inequalities hold:

$$\begin{aligned} \vec{\Xi}_1 &= \vec{\Gamma}_1^T \vec{P}_1 \vec{\Gamma}_1 - \lambda_1 \vec{\Gamma}_2^T \vec{P}_1 \vec{\Gamma}_2 + \vec{\Psi}_1 \\ &- \vec{\Phi}_1^T \left(\vec{Z} / \tilde{\sigma}_1 \right) \vec{\Phi}_1 + \text{Sym} \left(\vec{T}_1 \vec{\Sigma}_1 \right) < 0, \\ \vec{\Xi}_2(d) &= \begin{bmatrix} 1 & \vec{\Omega}(d) \\ \vec{\Omega}(d)^T & \text{diag}\{\vec{P}, 0\} + \vec{\Psi}_2 / \lambda_1 \end{bmatrix} \geq 0. \end{aligned}$$

where

$$\begin{aligned} \vec{\Omega}(l) &= \left[\vec{D}(l) \ \vec{G}(l) \ \vec{O}(l) \right], \\ \vec{\Gamma}_1 &= \begin{bmatrix} I & 0 & 0 & I \\ \kappa I & -I & I & 0 \end{bmatrix}, \\ \vec{\Gamma}_2 &= [I \ 0 \ 0 \ 0], \vec{\Phi}_1 = [\kappa I \ -I \ 0 \ 0], \\ \vec{\Gamma}_2 &= \begin{bmatrix} I & 0 & 0 & 0 \\ 0 & 0 & I & 0 \end{bmatrix}, \vec{\Phi}_1 = [\kappa I \ -I \ 0 \ 0], \\ \vec{\Sigma}_1 &= \left[(\vec{A} + \vec{L} - I) X^T + \vec{B} (E_y^- D + E_y Y) \right. \\ &\quad \left. \vec{A}_d X^T + \vec{B} E_y^- \vec{G} \ \vec{B} E_y^- \vec{O} \ -X^T \right], \\ \vec{\Psi}_1 &= \text{diag}\{\kappa \vec{S}_1 + \sigma \vec{S}_2, \vec{S}_1 / \tilde{\kappa}_1, \vec{S}_2 / \tilde{\sigma}_1, \sigma \vec{Z}\}, \\ \vec{\Psi}_2 &= \text{diag}\{0, \vec{S}_2 / \tilde{\sigma}_1, \vec{S}_1 / \tilde{\kappa}_1\} + (1 / \tilde{\sigma}_1) \\ &\quad \times \begin{bmatrix} \kappa^2 \vec{Z} & 0 & \kappa \vec{Z} \\ 0 & 0 & 0 \\ -\kappa \vec{Z} & 0 & -\vec{Z} \end{bmatrix}. \end{aligned}$$

Then, for any initial condition $\phi(\theta) \in [0, +\infty)$, $V_2(0) \leq 1$, the CLSEs (51) are exponentially bounded, and the corresponding synchronization controller can be determined by $K = YX^{-T}$.

Proof. Corollary 13 can be proved along a similar line to the proof of Theorem 10 and Theorem 11. Thus, the proof is omitted here.

4. NUMERICAL SIMULATIONS

In this section, two illustrative examples are provided for CCPNs to demonstrate the effectiveness of the presented synchronization control scheme.

Example 14. Consider a class of CCPNs with the form (1), which is composed of three identical nodes with the inner-coupling matrix $\Gamma = 0.517I$ and the following parameters:

$$A = \begin{bmatrix} 1.10 & 0.15 \\ 0.03 & 0.80 \end{bmatrix}, A_d = \begin{bmatrix} 1 & -0.1 \\ 0 & 1 \end{bmatrix},$$

$$B = \begin{bmatrix} 1 & 0.1 \\ 0.1 & 1 \end{bmatrix}, \mu_i = 2^{-i},$$

$$\bar{u}_1 = 15, 1 \leq \tau_k = 2 + (-1)^k \leq 3.$$

where the time-delay boundaries are set as $\tau_m = 0$, $\tau_M = 4$. Furthermore, the coupling matrix is selected as

$$L = \begin{bmatrix} -0.65 & 0.1 & 0.55 \\ 0 & -0.05 & 0.05 \\ 0.5 & 0 & -0.5 \end{bmatrix}.$$

Suppose that the FDI attacks have the following form:

$$f(u_i(k - \tau_k)) = \begin{bmatrix} \tanh(0.8u_{i1}(k - \tau_k)) \\ -\tanh(0.8u_{i2}(k - \tau_k)) \end{bmatrix},$$

and according to Assumption 1, let $F = \text{diag}\{0.8, -0.8\}$. The initial conditions of CCPNs are set as $x_1(0) = [2 \ 2]$, $x_2(0) = [-2 \ -2]$, and $x_3(0) = [1 \ 1]$, respectively. Then, the FDI attacks' energy evolution is shown in Fig. 2, as well as Fig. 3 and Fig. 4 plot synchronization error trajectories of the uncontrolled, which demonstrates that the CCPNs cannot be spontaneously synchronized.

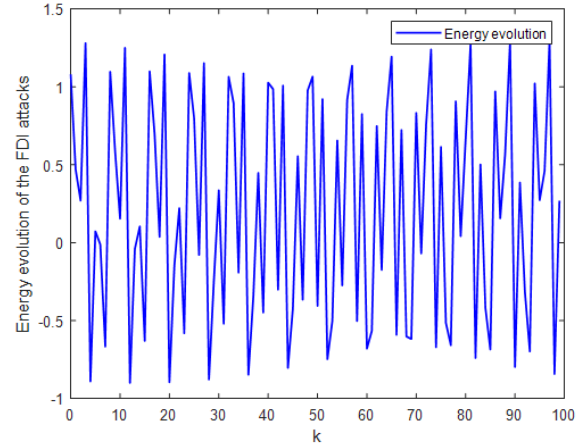


Fig. 2. Energy evolution of the FDI attacks.

Let the parameters be $\delta_1 = \delta_2 = \delta_3 = 4$, $\lambda_1 = 1$, $\lambda_2 = 1.24$ and $\pi = 0.97$. By applying Theorem 11 and solving LMIs (45)-(50), we have the following the synchronization controller gains:

$$K_1 = \begin{bmatrix} -3.3160 & -0.3418 \\ -0.2554 & -0.0394 \end{bmatrix},$$

$$K_2 = \begin{bmatrix} 1.0695 & 0.1026 \\ 0.4586 & 0.0398 \end{bmatrix},$$

$$K_3 = \begin{bmatrix} 0.5240 & 0.0463 \\ 1.6202 & 0.1603 \end{bmatrix}.$$

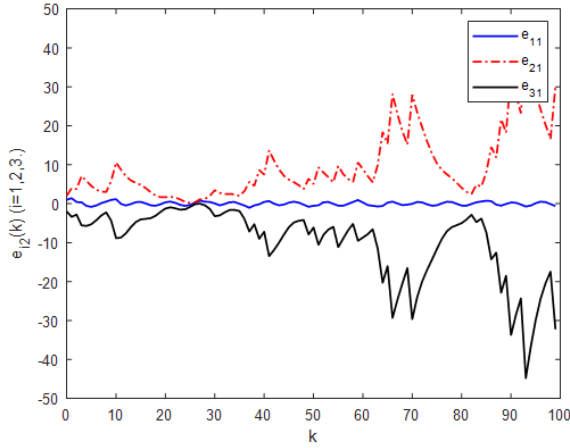


Fig. 3. Synchronization error $e_{i1}(k)$, ($i = 1, 2, 3$) trajectories of the uncontrolled.

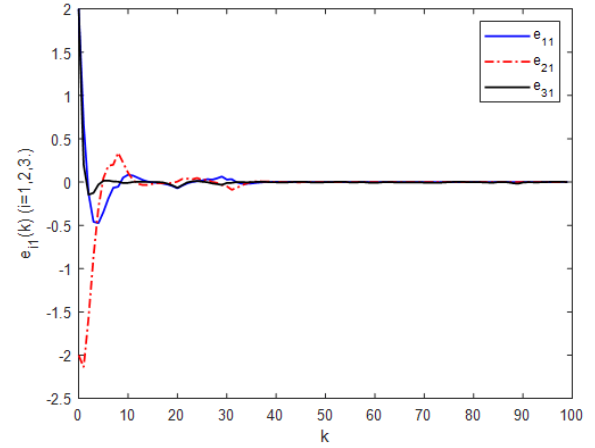


Fig. 5. Synchronization error $e_{i1}(k)$, ($i = 1, 2, 3$) trajectories of the controlled.

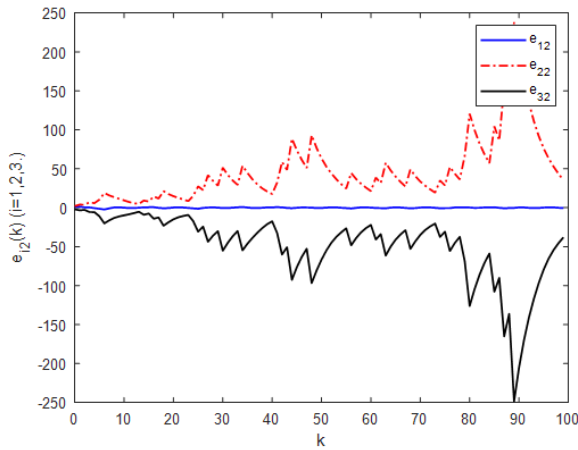


Fig. 4. Synchronization error $e_{i2}(k)$, ($i = 1, 2, 3$) trajectories of the uncontrolled.

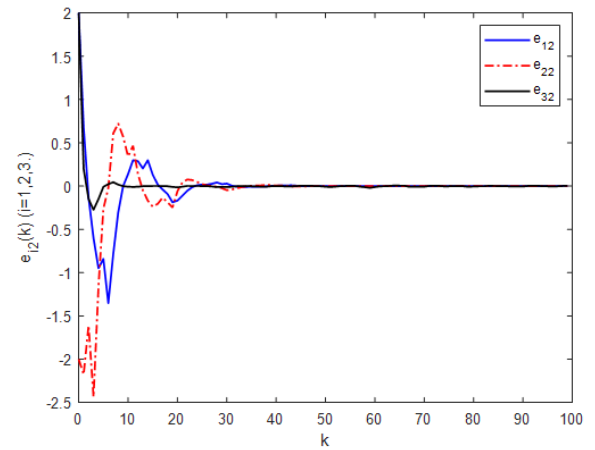


Fig. 6. Synchronization error $e_{i2}(k)$, ($i = 1, 2, 3$) trajectories of the controlled.

In this case, Fig. 5 and Fig. 6 show the synchronization error trajectories of CCPNs, respectively. The proposed synchronization controller could render synchronization errors to be converged for CCPNs, which means that the proposed method is effective. Fig. 7 and Fig. 8 show the synchronization error trajectories of CCPNs under FDI attacks, respectively. It could be found from Fig. 7 and Fig. 8 that the proposed synchronization controller is still effective for CCPNs under FDI attacks and mixed delays, but there are some fluctuations in the synchronization error trajectories. To demonstrate the superiority of the proposed control method. Fig. 9 and Fig. 10 plot the synchronization error trajectories under the sampled-data synchronization control method of Lee and Park (2019) for CCPNs (1) in the same initial conditions. It could be found from Fig. 7-Fig. 10 that the proposed synchronization control method of this paper can effectively alleviate the multiple effects of the FDI attacks and mixed delays with lower synchronization error fluctuations, which indicates the superiority of the proposed synchronization control method.

Example 15. Consider CCPNs (1) that consist of three unmanned vehicles Guan et al. (2019) with the following parameters:

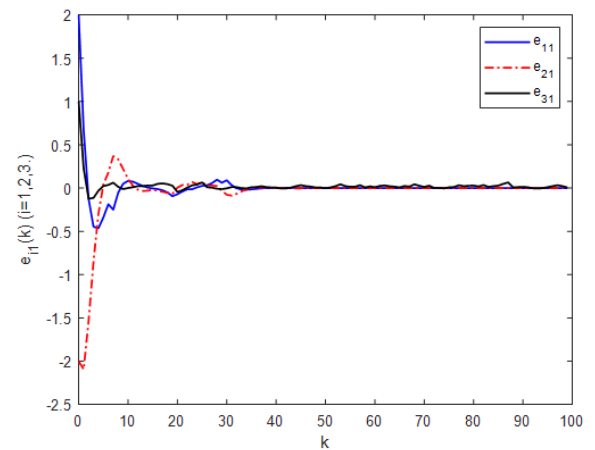


Fig. 7. Synchronization error $e_{i1}(k)$, ($i = 1, 2, 3$) trajectories of the controlled under FDI attacks.

$$A = \begin{bmatrix} 0 & -3.3275 \\ 3.6189 & 0 \end{bmatrix}, B = \begin{bmatrix} 4.8987 & 0.1442 \\ 3.8424 & 0.8803 \end{bmatrix},$$

The inner-coupling matrix is set as $\Gamma = 0.517I$, and the outer-coupling matrices L is given as follows:

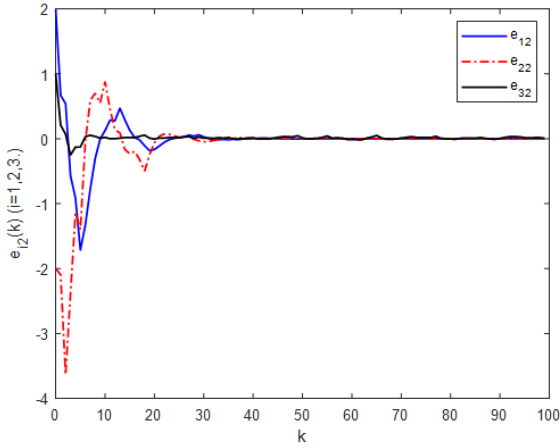


Fig. 8. Synchronization error $e_{i2}(k)$, ($i = 1, 2, 3$) trajectories of the controlled under FDI attacks.

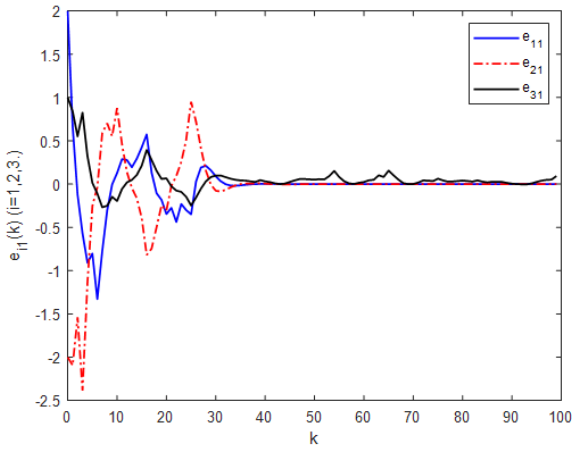


Fig. 9. Synchronization error $e_{i1}(k)$, ($i = 1, 2, 3$) trajectories of the control method in Lee and Park (2019).

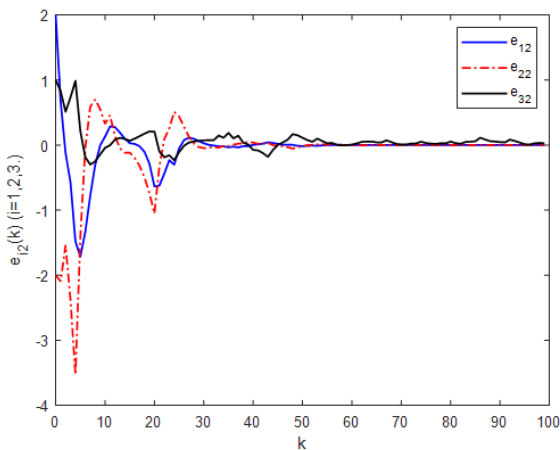


Fig. 10. Synchronization error $e_{i2}(k)$, ($i = 1, 2, 3$) trajectories of the control method in Lee and Park (2019).

$$L = \begin{bmatrix} -0.1 & 0 & 0.1 \\ 0 & -0.1 & 0.1 \\ 0.1 & 0.1 & -0.2 \end{bmatrix}.$$

Other parameters of CCPNs are the same as in Example 14. By applying Theorem 11 and solving LMIs (45)-(50), we have the following the synchronization controller gains:

$$K_1 = \begin{bmatrix} 0.1647 & 0.4911 \\ -0.0796 & -0.2374 \end{bmatrix},$$

$$K_2 = \begin{bmatrix} 0.1689 & 0.5017 \\ -0.0501 & -0.1489 \end{bmatrix},$$

$$K_3 = \begin{bmatrix} 0.1710 & 0.4981 \\ -0.0646 & -0.1881 \end{bmatrix}.$$

The initial conditions of CCPNs are same as in Example 14. In this case, the trajectories of synchronization error between the three unmanned vehicles are shown in Fig. 11 and Fig. 12, respectively. It could be found from Fig. 11 and Fig. 12 that the synchronization errors of three unmanned vehicles converge to zero within the limited sampling periods, which implies that the presented synchronization control method is effective for the multi-unmanned vehicles with mixed delays under FDI Attacks.

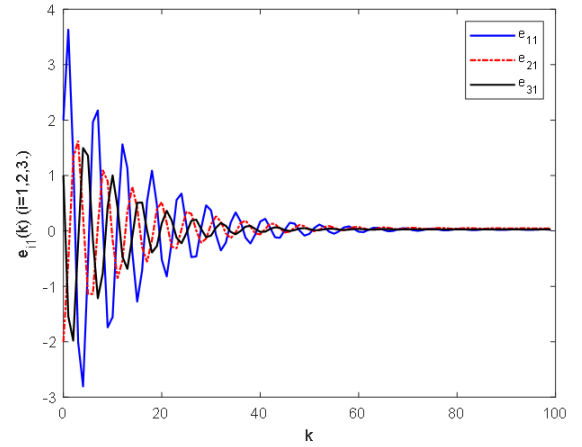


Fig. 11. Synchronization error $e_{i1}(k)$, ($i = 1, 2, 3$) trajectories of the controlled under FDI attacks.

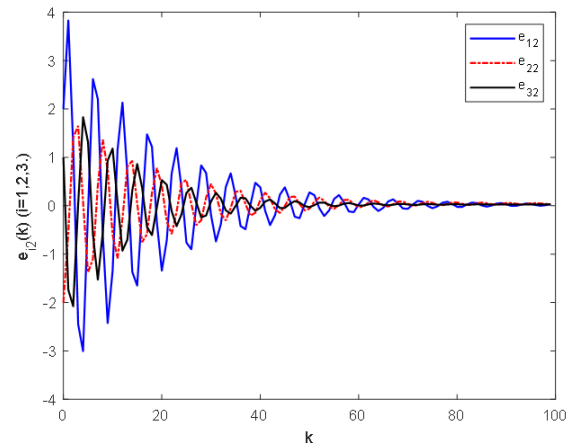


Fig. 12. Synchronization error $e_{i2}(k)$, ($i = 1, 2, 3$) trajectories of the controlled under FDI attacks.

5. CONCLUSION

The purpose of the current study is to investigate the synchronization control problem for CCPNs under FDI attacks. Firstly, an innovative polytopic model is proposed to describe the effects of FDI attacks and input delays, and then the model of CLSEDs is established. Secondly, sufficient conditions are derived by using appropriate Lyapunov-like function and summation inequalities, and the synchronization control gain is obtained for ensuring that the CLSEDs are ultimately exponentially bounded. Finally, a numerical example is given to verify the effectiveness and superiority of the proposed synchronization control method. In the future, the discontinuous synchronization control scheme will be investigated to further reduce the control costs of CCPNs under cyber attacks.

ACKNOWLEDGEMENTS

The authors gratefully acknowledge the financial supports by the National Science Foundation of China under Grant 62363024 and 62263019, as well as the Science and Technology Program of Gansu Province under Grant 21ZD4GA028.

REFERENCES

- Barboni, A., Boem, F., and Parisini, T. (2018). Model-based detection of cyber-attacks in networked mpc-based control systems. *IFAC-PapersOnLine*, 51(24), 963–968.
- Cetinkaya, A., Ishii, H., and Hayakawa, T. (2015). Event-triggered output feedback control resilient against jamming attacks and random packet losses. *IFAC-PapersOnLine*, 48(22), 270–275.
- Chen, Y. and Wang, Z. (2020). Local stabilization for discrete-time systems with distributed state delay and fast-varying input delay under actuator saturations. *IEEE Transactions on Automatic Control*, 66(3), 1337–1344.
- Chen, Y., Wang, Z., Fei, S., and Han, Q.L. (2018). Regional stabilization for discrete time-delay systems with actuator saturations via a delay-dependent polytopic approach. *IEEE Transactions on Automatic Control*, 64(3), 1257–1264.
- Chen, Y., Wang, Z., Hu, J., and Han, Q.L. (2020). Synchronization control for discrete-time-delayed dynamical networks with switching topology under actuator saturations. *IEEE Transactions on Neural Networks and Learning Systems*, 32(5), 2040–2053.
- Fu, W., Qin, J., Shi, Y., Zheng, W.X., and Kang, Y. (2019). Resilient consensus of discrete-time complex cyber-physical networks under deception attacks. *IEEE Transactions on Industrial Informatics*, 16(7), 4868–4877.
- Gao, W., Wu, H., Siddiqui, M.K., and Baig, A.Q. (2018). Study of biological networks using graph theory. *Saudi journal of biological sciences*, 25(6), 1212–1219.
- Guan, Y., Wu, Y., Wu, H., Li, Y., and He, S. (2019). Synchronization of complex dynamical networks with actuator saturation by using sampled-data control. *Circuits, Systems, and Signal Processing*, 38(12), 5508–5527.
- He, W., Gao, X., Zhong, W., and Qian, F. (2018). Secure impulsive synchronization control of multi-agent systems under deception attacks. *Information Sciences*, 459, 354–368.
- Ju, Z., Zhang, H., and Tan, Y. (2020). Distributed deception attack detection in platoon-based connected vehicle systems. *IEEE transactions on vehicular technology*, 69(5), 4609–4620.
- Kazemy, A., Saravanakumar, R., and Lam, J. (2021). Master-slave synchronization of neural networks subject to mixed-type communication attacks. *Information Sciences*, 560, 20–34.
- Lee, T.H. and Park, J.H. (2019). Design of sampled-data controllers for the synchronization of complex dynamical networks under controller attacks. *Advances in Difference Equations*, 2019(1), 1–15.
- Mousavinejad, E., Yang, F., Han, Q.L., Ge, X., and Vlacic, L. (2019). Distributed cyber attacks detection and recovery mechanism for vehicle platooning. *IEEE Transactions on Intelligent Transportation Systems*, 21(9), 3821–3834.
- Musleh, A.S., Chen, G., and Dong, Z.Y. (2019). A survey on the detection algorithms for false data injection attacks in smart grids. *IEEE Transactions on Smart Grid*, 11(3), 2218–2234.
- Peng, C., Sun, H., Yang, M., and Wang, Y.L. (2019). A survey on security communication and control for smart grids under malicious cyber attacks. *IEEE Transactions on Systems, Man, and Cybernetics: Systems*, 49(8), 1554–1569.
- Qu, Y. and Pang, K. (2020). State estimation for a class of artificial neural networks subject to mixed attacks: A set-membership method. *Neurocomputing*, 411, 239–246.
- Rakkiyappan, R., Cao, J., and Velmurugan, G. (2014). Existence and uniform stability analysis of fractional-order complex-valued neural networks with time delays. *IEEE Transactions on Neural Networks and Learning Systems*, 26(1), 84–97.
- Seuret, A., Gouaisbaut, F., and Fridman, E. (2015). Stability of discrete-time systems with time-varying delays via a novel summation inequality. *IEEE Transactions on Automatic Control*, 60(10), 2740–2745.
- Shi, D., Guo, Z., Johansson, K.H., and Shi, L. (2017). Causality countermeasures for anomaly detection in cyber-physical systems. *IEEE Transactions on Automatic Control*, 63(2), 386–401.
- Shi, K., Zhong, S., Tang, Y., Cheng, J., et al. (2020). Hybrid-driven finite-time H_∞ sampling synchronization control for coupling memory complex networks with stochastic cyber attacks. *Neurocomputing*, 387, 241–254.
- Solomon, O. and Fridman, E. (2013). New stability conditions for systems with distributed delays. *Automatica*, 49(11), 3467–3475.
- Souza, F.d.O., Mozelli, L.A., de Oliveira, M.C., and Palhares, R.M. (2016). Lmi designmethod for networked-based pid control. *International Journal of Control*, 89(10), 1962–1971.
- Srinivasan, G., Kumar, R.S., and Muthukaruppasamy, S. (2022). Evaluation of additional power loss reduction in dg integrated optimal distribution network. *Journal of Control Engineering and Applied Informatics*, 24(1), 68–75.

- Tan, S., Guerrero, J.M., Xie, P., Han, R., and Vasquez, J.C. (2020). Brief survey on attack detection methods for cyber-physical systems. *IEEE Systems Journal*, 14(4), 5329–5339.
- Wen, G., Yu, W., Yu, X., and Lü, J. (2017). Complex cyber-physical networks: From cybersecurity to security control. *Journal of Systems Science and Complexity*, 30(1), 46–67.
- Zafar, R., Mahmood, A., Razzaq, S., Ali, W., Naeem, U., and Shehzad, K. (2018). Prosumer based energy management and sharing in smart grid. *Renewable and Sustainable Energy Reviews*, 82, 1675–1684.
- Zhou, B. (2013). Analysis and design of discrete-time linear systems with nested actuator saturations. *Systems & Control Letters*, 62(10), 871–879.
- Zhou, L., Huang, M., Tan, F., and Zhang, Y. (2023). Mean-square bounded synchronization of complex networks under deception attacks via pinning impulsive control. *Nonlinear Dynamics*, 1–17.